THE JOURNAL OF PHYSICAL CHEMISTRY C

Article

Cite This: J. Phys. Chem. C 2018, 122, 7968−7974

pubs.acs.org/JPCC

Size Effect on the High-Strength and Electrically Conductive Polyolefin/Reduced Graphene Oxide (RGO) Composites

Wensheng Gao,[†] Huqiang Chen,[†] Jiandong Cao,[†] Songbo Chen,[†] Yu Ma,[‡] Qinjia Chen,[†] Bochao Zhu,[§] Junji Jia,[§] Anping Huang,[§] and Yongxiao Bai*[,†]

[†]MOE Key Laboratory for Magnetism and Magnetic Materials, Institute of Material Science and Engineering, Lanzhou University, Lanzhou 730000, P. R. China

[‡]Department of Chemical Engineering and Biointerfaces Institute, University of Michigan, Ann Arbor, Michigan 48109-2136, United States

[§]Lanzhou Petrochemical Research Center, Petro china Lanzhou 730000, P. R. China

* Supporting Information

ABSTRACT: Size-controlled alkylated reduced graphene oxide (M-LTRGO) with a narrow particle size distribution was synthesized in one step via a low-temperature thermal expansion strategy at a large scale. The physicochemical properties of the modified graphite oxide (M-GO) and M-LTRGO with changes in the particle size were characterized and discussed. After incorporation in low-density linear polyethylene (LLDPE) by melt blending, the composites have been characterized regarding their morphological, mechanical, and electrical properties to study the performance evolution of LLDPE/M-LTRGO with changing M-LTRGO size. The electrical properties of the LLDPE/M-LTRGO composites show the exact opposite trend with the M-LTRGO tablet, as the changing of the average M-LTRGO size. The opposite electrical phenomenon ascribes the small-size M-LTRGO resulting in a better dispersion in LLDPE matrix, which is determined by the mean surface-to-surface interparticle distance (IPD) from examination of scanning electron micrographs.

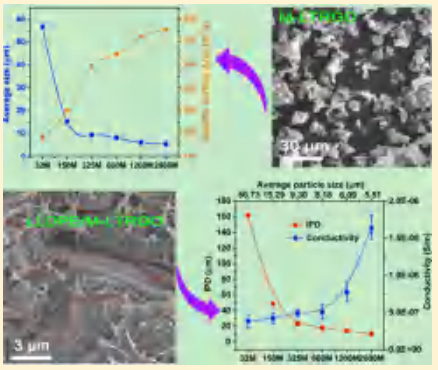

INTRODUCTION

The high plastic conductive composites have received increasing attentions recently due to persistent conductive pathways when stretched, bended, twisted, or folded, which provides great potential in the field of sensors, stretchable electronics, conductive adhesives, etc.[1] Polymer nanocomposites based on carbon black, carbon nanotubes, and nanometal particles have been used for improved mechanical and electrical properties and environmental applications of polymers.[2,3]The discovery of graphene[4] with its combination of extraordinary physical properties and ability to be dispersed in various polymer matrices has created a new class of conductive polymer nanocomposites.[5] Among them, polyolefin composites have been developing vigorously to overcome some drawbacks of pure polyolefin,[1,6] which is the most widely used polymer[7] in human life and industrial manufacturing due to the outstanding properties, such as easy processing, chemical stability, nontoxicity, and low cost.[8,9] Recently, thanks to the development of effective chemical and thermal reduction methods of graphite oxide (GO), large scale preparation of reduced graphene oxide (RGO) has been rapidly developed to fulfill the mass demand in the conductive polyolefin composites field[6,10,11] due to relatively more excellent physical properties.[12−16] The physicomechanical properties of a polyolefin-based RGO composite are highly dependent on the dispersion state and interfacial interaction between RGO and polyolefin.[17,18] However, there are no polar groups on the backbone of LLDPE, which restricts the effective dispersion and interface compatibility of RGO without compatibilization.[19,20] The functionalization of RGO is relatively complex and difficult for wide industrial production. Normally, the GO was first low-temperature exfoliated[12] into high-exfoliated RGO to retain more functional groups, followed by further functionalization to improve the interfacial compatibility, such as LLDPE-graft-Aminomethylpyridine/RGO,[21] Polypropylene-graft-thermally RGO,[22] etc. These synthetic strategies significantly enhance the electrical and thermal properties of the polyolefin/RGO composites depending on the high pre-exfoliation and effective alkyl modification to RGO, but the complex synthesis process is still not concise enough to meet the demand of industry production. Herein, the in situ peeling modified GO provides with us a facile route to synthesize high-exfoliated functional RGO at large scale.[6,23] The efficient and environmentally friendly modifier is the key issue to fabricating the high-exfoliated functional RGO at large scale. The dodecyldimethylamine oxide (DDAO) as an amine oxide based zwitterionic surfactant is one of the most frequently

Received: December 29, 2017
Revised: February 22, 2018
Published: March 22, 2018

DOI: 10.1021/acs.jpcc.7b12787
J. Phys. Chem. C 2018, 122, 7968−7974

Scheme 1. Schematic Illustrating a Procedure To Fabricate LLDPE/M-LTRGO Composites

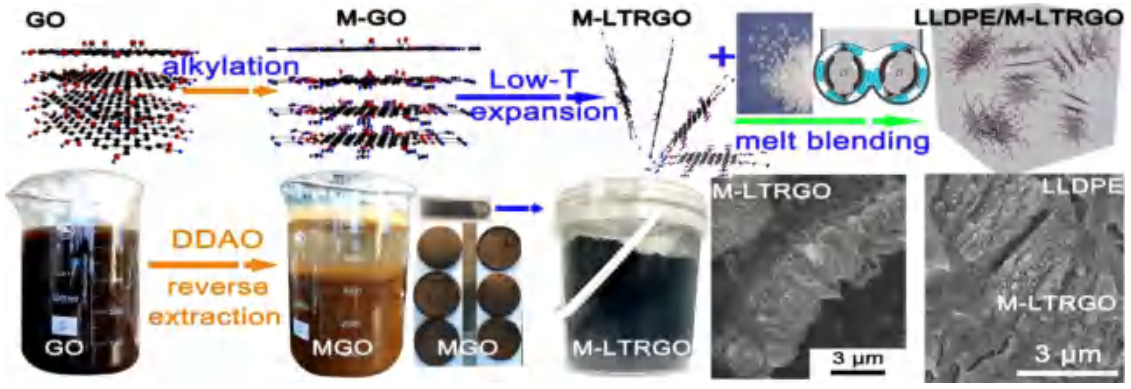

used surfactants and widely used in detergent, toiletry, and antistatic preparations,[24] which was capable of being rapidly grafted on the surface of GO in acidic and neutral aqueous solution and showed excellent lipophilicity.[19] It is worth mentioning that amine oxide based surfactants (include DDAO) could be rapidly and easily converted into carbon dioxide, water, and biomass under aerobic conditions without secondary pollution to the environment.[25]

In this work, size-controlled GO was first alkylated with DDAO in aqueous solution, which not only accelerates the drying process due to the excellent hydrophobicity but also constructs a spacer between the GO particles. Then the size-controlled alkylated GO (M-GO) was thermally expanded at low temperature into the size-controllable modified low-temperature reduced graphene oxide (M-LTRGO) with a narrow particle size distribution. After incorporation in LLDPE by melt blending, the composites have been characterized regarding their morphological, mechanical, and electrical properties to study the performance evolution of LLDPE/M-LTRGO with changing particle size. The inner connection between the physicochemical properties of composites and the size of the M-LTRGO was assessed by determining the mean surface-to-surface interparticle distance (IPD)[26] from an examination of scanning electron micrographs. The designed RGO has built-in alkyl functions that facilitate novel material processing and diverse applications.[27,28] The large specific surface area, open 3D structure, high conductivity, and chemical activity may turn M-LTRGO into a high-capacity well-ordered ion storage medium that is feasible for applications concerning supercapacitors,[12,23] lithium-ion batteries,[29] ect.

METHODS

The synthesis of size-controllable M-LTRGO involves three steps (Scheme 1). The first results in fully oxidized graphite with a modified Hummers method[30] as the raw material of the flaky graphite with optimized mesh (including 32, 150, 325, 600, 1200, 2000 mesh). The second corresponds with the rapid alkyl modification to GO. The excessive dodecyldimethylamine oxide (DDAO) was slowly added into the above designed graphite oxide (GO) suspension with the assistance of mechanical agitation. Then, the GO rapidly flocculated and deposited. Eventually, the modified graphite oxide (M-GO) was washed by suction filtration and dried at 60 °C for 24 h. The last step is responsible for the low-temperature thermal exfoliation to MGO with modified low-temperature expansion technology.[6] The LLDPE/M-LTRGO composites were prepared by melt blending using a Lab Tech melt mixer at 180 °C for 15 min at the rotor speed of 60 r/min. Finally, test samples were obtained by hot-press forming technology at 180 °C/15 MPa for 10 min.

Characterization of Structure and Components. Elemental composition was carried on the X-ray photoelectron spectrum (XPS, ESCALAB 250), and a liner background was assumed. The monography and structure were investigated by Scanning Electron Microscopy (SEM-Tescan MIRA 3 XMU/XMH), transmission electron microscopy (TEM-Hitachi H-600), and X-ray diffraction patterns (XRD-Rigaku D/max-2400). The surface area and pore structure of the samples were measured by N_2 adsorption at 77 K using the BET method on a MICROMERITICS TriStarII 3020 surface analyzer. Thermal gravimetric analysis (TGA) of the samples was performed on a Perkin−Elmer Diamond thermal analyzer from room temperature to 700 °C, using a heating rate of 10 °C/min with Ar protection. The tensile strength of the designed samples was tested according to the China National Standard GB/T 1040.2−2006 with a tensile rate of 50 mm/min. The electrical conductivity of the M-GO and LLDPE/M-LTRGO composites were measured by a PC68 digital high resistance meter (Shanghai No.6 Electric Meter Factory Co., Ltd. China). The electrical conductivity of the M-LTRGO is measured by a Four-Prober.

RESULTS AND DISCUSSION

The physicomechanical properties of the polymer composites are mainly determined by the dispersion state of the filler and interfacial interaction between the filler and polymer matrix.[17,18] In order to improve the dispersion of RGO in the polyolefin matrix during the melt blending, the exfoliation to RGO is believed to be necessary to increase the contract surface and molecular chains wetting rate.[6,16,21,31] As shown in Figure 1a, after low temperature thermal expansion, the MGO was exfoliated into the accordion-like 3D structure with a large specific surface area of about 300 m^2/g. It exhibits the type-IV adsorption isotherms[32] from the adsorption−desorption curve as shown in Figure 1b. Similar to the SEM image in Figure 1a, the adsorption model of M-LTRGO shows good consistency with the combination of the ink bottle structure[33] and V-plate structure[32] through fitting the adsorption/desorption curve. Simultaneously, the size-controllable M-LTRGO was successfully synthesized by optimizing the size of the raw graphite as shown in Figure 2.

As observed from the size statistics of size-controlled M-LTRGO, the size of the M-LTRGO decreases with decreasing graphite size; the size of all the M-LTRGO is generally less than

DOI: 10.1021/acs.jpcc.7b12787
J. Phys. Chem. C 2018, 122, 7968−7974

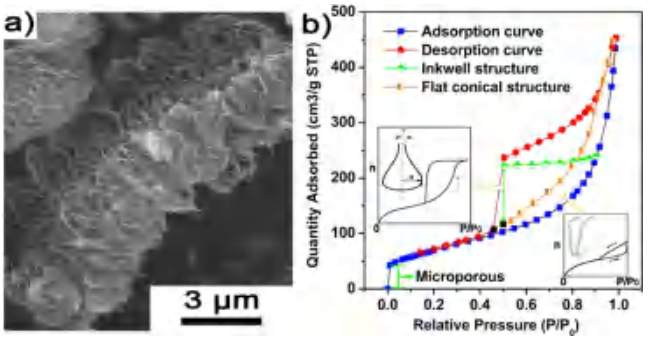

Figure 1. Morphological characterization (a) and adsorption behavior (b) of M-LTRGO.

the raw graphite due to the violent oxidation and low-temperature expansion reduction. Correspondingly, as shown in Figure 3a, the specific surface area (SSA) of the M-LTRGO gradually increases with the decrease in the M-LTRGO average size, as further supported by the adsorption−desorption curve in Figure 3b. The SSA value behaves in a linear relationship with the reciprocal of the average size (1/R) of M-LTRGO as shown in following eq 1:

$$\mathrm{SSA}\ (\mathrm{m}^2/\mathrm{g}) = 187.7 + 600 \Big/ R_{\mathrm{average}}\ (\mu\mathrm{m}) \quad (1)$$

Besides the effect of filler dispersion on the performance of composites, the interfacial interactions between M-LTRGO and the polyolefin matrix plays an important role in maximizing the physical properties of RGO.[34] Therefore, the GO was first modified by the DDAO in an extremely short time (5−30 s), with further low-temperature thermal exfoliation to M-LTRGO with short alkyl chains on the surface as shown in the inset schematic of Figure 4a, which is beneficial in increasing the compatibility between M-LTRGO and the polyolefin matrix.[17,19] As shown in Figure 4a, the peaks that appeared at 3437, 1632, and 1066 cm^{-1} in the FT-IR spectrum of M-

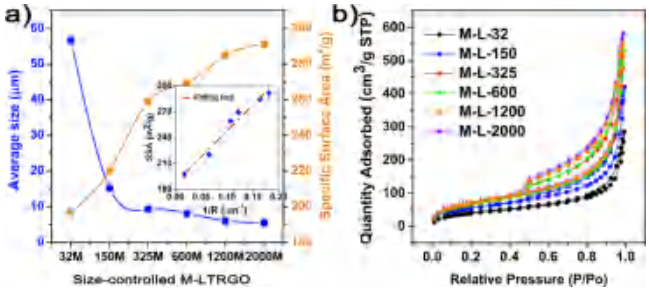

Figure 3. Size statistics and BET analysis of size-controlled M-LTRGO.

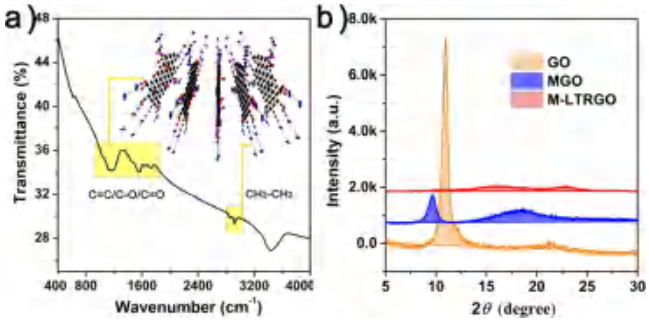

Figure 4. FT-IR spectrum (a) and XRD pattern (b) of M-LTRGO.

LTRGO are a typical feature of GO/RGO, corresponding to the presence of hydroxyl, carboxyl, and epoxy groups, respectively.[12] Besides, the asymmetric peak relative intensity of M-LTRGO at 2920 and 2845 cm^{-1} were assigned to the CH_2 stretching vibrations of the alkyl group.[35] It was sufficient to provide good dispersion and high interfacial adhesion between the RGO sheets and LLDPE matrix. Simultaneously, as shown in Figure 4b, the disappearance of the X-ray feature diffraction peak of MGO of about 9.28° demonstrates the full exfoliation to MGO.[12,36]

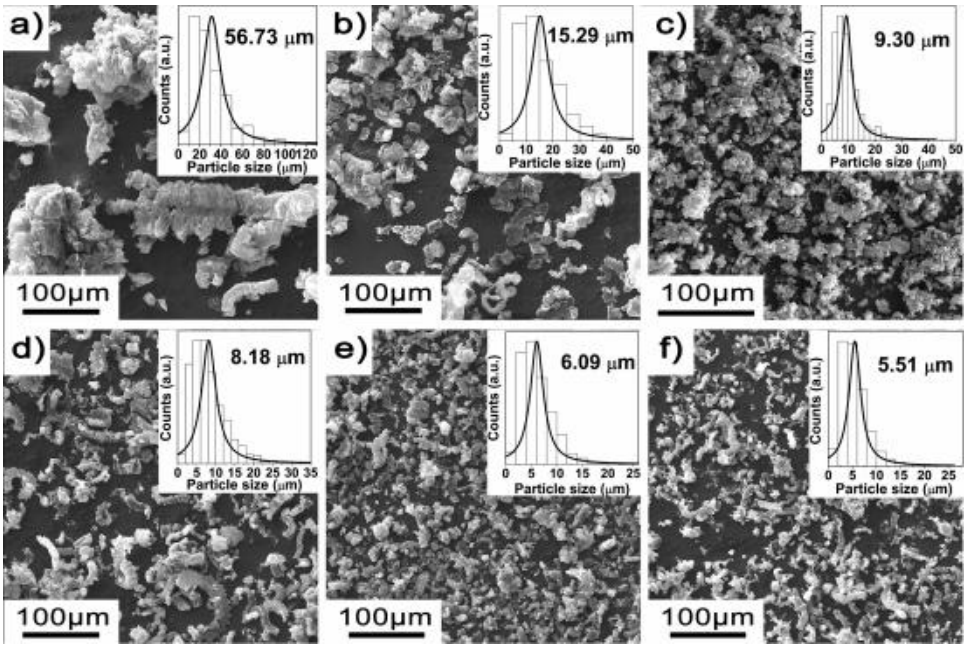

Figure 2. SEM characterization and horizontal size statistics of size-controlled M-LTRGO corresponding to the raw graphite size of 32M (a), 150M (b), 325M (c), 600M (d), 1200M (e), and 2000M (f), respectively.

DOI: 10.1021/acs.jpcc.7b12787
J. Phys. Chem. C 2018, 122, 7968−7974

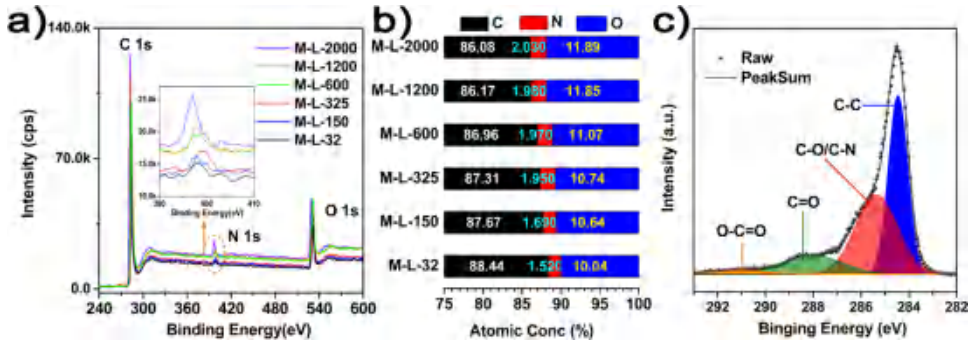

Figure 5. XPS wide spectrum (a), atomic concentration ratio (b), and fine fitting spectrum of M-LTRGO (c).

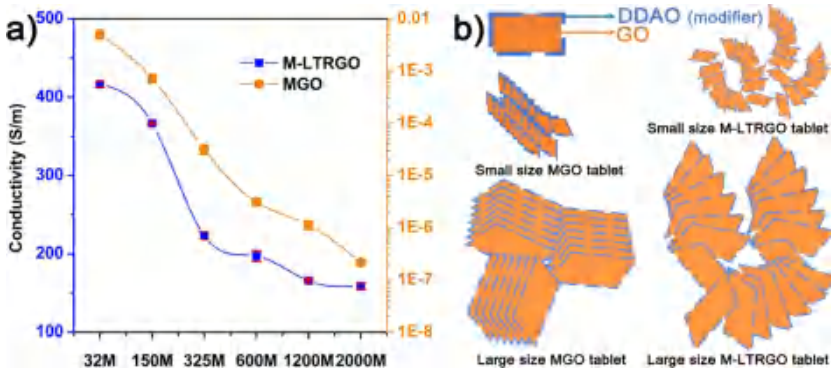

Figure 6. Electrical behavior of MGO and M-LTRGO with gradient size.

After further characterization by an X-ray photoelectron spectrometer (XPS), the N element (identifier element of DDAO) concentration ratio gradually increases with the decreasing average size of M-LTRGO, as shown in Figure 5a, b. This is because that there would be more DDAO alkyl chains attached on the surface of the smaller size MGO particle due to the size effect, processing higher content in unit volume. In addition, the C−N bond (285.6 ± 0.3 eV) of the C 1s fitting spectrum (Figure 5c) certifies that a certain amount of alkyl groups attach on the surface of M-LTRGO.[37]

The modifier concentration on the surface of L-LTRGO would affect the electrical behavior of the MGO and M-LTRGO,[16] as shown in Figure 6a. Generally, the volume electrical conductivity of the MGO and M-LTRGO compressed tablets (20 MPa, 10 min) gradually decreases with the decreasing average size of the samples. From comparision of MGO and M-LTRGO with the GO and RGO, it was observed that the modifier (DDAO) is the isolated phase because of the poor electrical conductivity. So increasing the isolated phase and decreasing the conductive phase in the compressed MGO and M-LTRGO film collaboratively led to the decreasing volume conductivity, which is also supported by the XPS characterization (Figure 5). Before thermal exfoliation, the electrical conductivity of MGO shows a decline in magnitude with the decreasing average size of MGO. Once thermally exfoliated, the electrical conductivity of M-LTRGO shows the same decreasing trend but within an order of magnitude. This is because, after rapid modification, the modifier (DDAO) is mainly concentrated on the surface of the MGO (without ultrasonic stripping) as shown in Figure 6b, compared with the exfoliated M-LTRGO, the isolated phase (DDAO) occupies more volume in the MGO tablet than M-LTRGO, and the M-LTRGO is easily able to achieve sheet contact. Therefore, the MGO finally shows a more significant changing trend than M-LTRGO in volume resistance.

To investigate the size effect of M-LTRGO in melt-blending polyolefin/RGO composites, the designed M-LTRGO was effectively incorporated in the LLDPE matrix relying on the expected alkyl modification and exfoliated 3D open structure. At a high concentration of M-LTRGO loading, the crystallinity of the LLDPE composites dynamically declines due to the steric effect and the thermal motion restricting polymer chains during the cooling crystallization process.[38] As shown in Figure 7a, the crystallinity of the LLDPE/M-LTRGO composites was calculated according to the following eq 2:[19]

$$X_c = \frac{S_{200} + S_{100}}{S_{200} + S_{100} + S_A} \quad (2)$$

The conductivity of the PPR/M-LTRGO composites was also characterized regarding the influence of the loadings (Figure S3) and size (Figure 7) of M-LTRGO. As shown in Figure 7b, the volume electrical conductivity of the LLDPE/M-

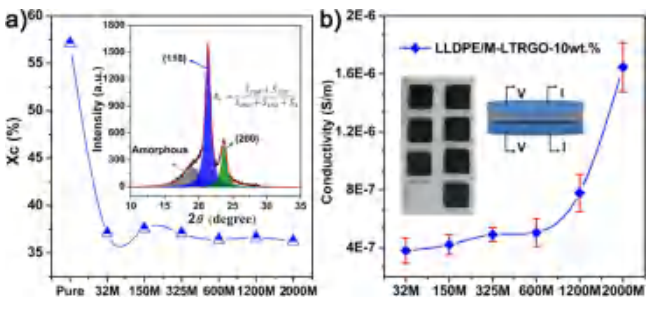

Figure 7. XRD patterns (a) and volume electrical conductivity (b) of LLDPE/M-LTRGO composites.

DOI: 10.1021/acs.jpcc.7b12787
J. Phys. Chem. C 2018, 122, 7968−7974

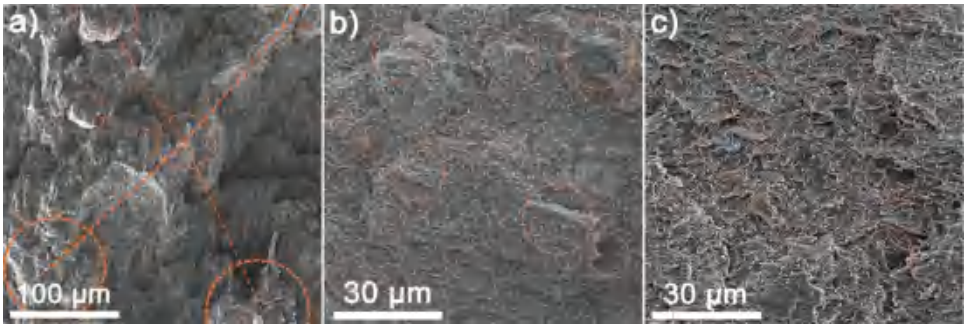

Figure 8. SEM images of LLDPE/M-LTRGO composites with M-LTRGO-phase highlighted in yellow, corresponding to (a) L/M-L-32 (large), (b) L/M-L-325 (middle), and (c) L/M-L-1200 (small).

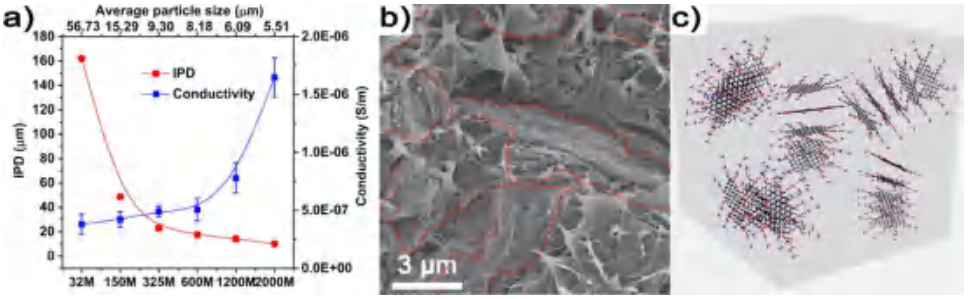

Figure 9. Interparticle distance (IPD) plotted as a function of M-LTRGO particle average size (a). Conductive network SEM image (b) and model diagram (c).

LTRGO composites gradually increases with decreasing M-LTRGO size, which varies in a contrasting trend to the electrical conductivity change of MGO and M-LTRGO. It could be explained from the dispersion of the M-LTRGO and the construction of the conductive network in LLDPE composites.

The loadings of 10 wt % in this system is enough to realize the construction of the conductive network for designed M-LTRGO as supported by the SEM characterizations (Figure 8) and electricity test results (Figure S3). Here, the dispersion of the M-LTRGO in the LLDPE matrix was assessed by determining the mean surface-to-surface interparticle distance (IPD)[26] from an examination of scanning electron micrographs. The much lower IPD in the surface-modified nanoparticle composite indicated a greater degree of dispersion and a higher interfacial surface area between the nanoparticles and the LLDPE matrix.[39]

As shown in Figure 8a, the M-LTRGO randomly distributes in the LLDPE matrix. The seamless convergence between M-LTRGO and LLDPE (Figure S2) indicates the good compatibility,[40] which is beneficial from the modification of DDAO. The large-size M-LTRGO still retains the generally larger shape, similar to the small-size M-LTRGO as shown in Figure 8 and Figure S2. By the statistical mean center-to-center distance of M-LTRGO in the matrix, the IPD in the LLDPE/M-LTRGO composites gradually decrease (from 160−10 μm) with the decrease in average size, which indicates a better particle dispersion[39] in the LLDPE matrix as shown in Figure 9a. Therefore, the correspondingly increased volume electrical conductivity of the LLDPE/M-LTRGO should be ascribed to the better particle dispersion of M-LTRGO, both exhibiting good correspondence in Figure 9a. As shown in Figure 9b, c, the electric conduction of the composite is realized on the basis of retaining the original morphology of the M-LTRGO and contacting each other. Therefore, the better M-LTRGO dispersion facilitates constructing more electric conductive channels in the LLDPE matrix and results higher volume electrical conductivity.[41]

Eventually, the mechanical properties of LLDPE/M-LTRGO composites were tested via the Instron testing system shown in Figure 10a. After incorporating 10 wt % M-LTRGO, the

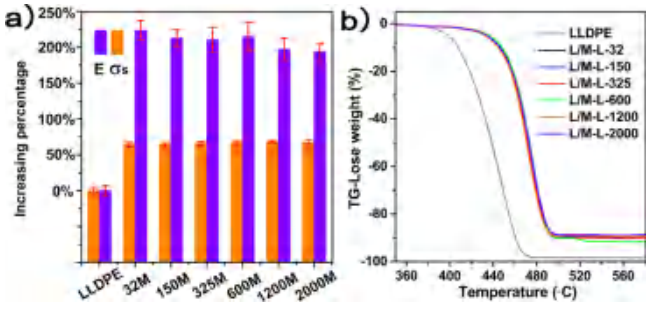

Figure 10. Mechanical properties (a) and thermal behaviors (b) of the LLDPE/M-LTRGO composites.

LLDPE/M-LTRGO composites display obvious enhancement in tensile yield strength (increased by 66% on average) and elastic modulus (increased by 210% on average) relying on the designed alkyl modification and open 3D structure,[42] which could provide the persistent conductive pathways under shock or a high load. The larger size M-LTRGO results in a higher modulus but a lower tensile yield strength in LLDPE/M-LTRGO composites through melt blending in this work. The lower tensile yield strength is due to the poorer dispersion of the large-size M-LTRGO in the LLDPE matrix; simultaneously, the higher elastic modulus is ascribed to the higher aspect ratio of large-size M-LTRGO.[43,44] Besides, as shown in Figure 10b, the obvious enhancement in thermal stability (increased 40 °C on average) effectively broadens the working temperature of

DOI: 10.1021/acs.jpcc.7b12787
J. Phys. Chem. C 2018, 122, 7968−7974

the electric conductive polyolefin composites.[45] It is still due to entanglement between RGO and LLDPE chains[22] and the high efficiency in catching free radicals.[46] The M-LTRGO can increase the thermal degradation activation energy of LLDPE/M-LTRGO nanocomposites through restricting the thermal motion of polymer chains.[38]

CONCLUSION

In summary, the M-LTRGO could significantly improve the mechanical (increased by 66% of tensile yield strength and 210% of elastic modulus) and electrical properties (increased by 7 orders of magnitude) as well as thermal stability (increased 40 °C on average) of the polyolefin/M-LTRGO relying on the open 3D structure and surface alkyl properties with a loading of 10 wt %. The larger-size M-LTRGO results a higher modulus but a lower tensile yield strength and a lower volume electrical conductivity in LLDPE/M-LTRGO composites due to the higher aspect ratio and poorer dispersion, respectively. The dispersion of the M-LTRGO in the LLDPE matrix was assessed by determining the mean surface-to-surface interparticle distance (IPD); the smaller size of the M-LTRGO results in the lower IPD and the better dispersion in LLDPE matrix. The volume electrical conductivity of the LLDPE/M-LTRGO increased with decreasing average size of the M-LTRGO mainly due to better particle dispersion.

ASSOCIATED CONTENT

* Supporting Information

The Supporting Information is available free of charge on the ACS Publications website at DOI: 10.1021/acs.jpcc.7b12787.

The relative characterization data are provided, including Raman spectrum characterization, section SEM images, and electrical conductivity of LLDPE/M-LTRGO composites (PDF)

AUTHOR INFORMATION

Corresponding Author

*Fax: +86-931-8910364. E-mail: baiyx@lzu.edu.cn.

ORCID

Yongxiao Bai: 0000-0001-5821-3015

Notes

The authors declare no competing financial interest.

ACKNOWLEDGMENTS

This work was supported by the Petro China Innovation Foundation (502000-071100003). We thank all the authors' contributions to this work.

REFERENCES

(1) Li, T.; Ma, L. F.; Bao, R. Y.; Qi, G. Q.; Yang, W.; Xie, B. H.; Yang, M. B. A New Approach to Construct Segregated Structures in Thermoplastic Polyolefin Elastomers Towards Improved Conductive and Mechanical Properties. J. Mater. Chem. A 2015, 3, 5482−5490.

(2) Kim, H.; Abdala, A. A.; Macosko, C. W. Graphene/Polymer Nanocomposites. Macromolecules 2010, 43, 6515−6530.

(3) Park, S.; Dikin, D. A.; Nguyen, S. T.; Ruoff, R. S. Graphene Oxide Sheets Chemically Cross-Linked by Polyallylamine. J. Phys. Chem. C 2009, 113, 15801−15804.

(4) Novoselov, K. S.; Geim, A. K.; Morozov, S. V.; Jiang, D.; Zhang, Y.; Dubonos, S. V.; Grigorieva, I. V.; Firsov, A. A. Electric Field Effect in Atomically Thin Carbon Films. Science 2004, 306, 666−669.

(5) Stankovich, S.; Dikin, D. A.; Dommett, G. H.; Kohlhaas, K. M.; Zimney, E. J.; Stach, E. A.; Piner, R. D.; Nguyen, S. T.; Ruoff, R. S. Graphene-Based Composite Materials. Nature 2006, 442, 282−286.

(6) Gao, W.; Li, J.; Yan, X.; Zhu, B.; Jia, J.; Huang, A.; Xie, K.; Bai, Y. Accordion-Like Graphene by a Facile and Green Synthesis Method Reinforcing Polyolefin Nanocomposites. RSC Adv. 2017, 7, 31085−31092.

(7) Kato, M.; Usuki, A.; Hasegawa, N.; Okamoto, H.; Kawasumi, M. Development and Applications of Polyolefin−and Rubber−Clay Nanocomposites. Polym. J. 2011, 43, 583−593.

(8) Koval'Chuk, A. A.; Shevchenko, V. G.; Shchegolikhin, A. N.; Nedorezova, P. M.; Klyamkina, A. N.; Aladyshev, A. M. Effect of Carbon Nanotube Functionalization on the Structural and Mechanical Properties of Polypropylene/Mwcnt Composites. Macromolecules 2008, 41, 7536−7542.

(9) Trujillo, M.; Arnal, M. L. A.; Müller, A. J.; Laredo, E.; Bredeau, S.; Bonduel, D.; Dubois, P. Thermal and Morphological Characterization of Nanocomposites Prepared by in-Situ Polymerization of High-Density Polyethylene on Carbon Nanotubes. Macromolecules 2007, 40, 6268−6276.

(10) Chen, W.; Yan, L. Preparation of Graphene by a Low-Temperature Thermal Reduction at Atmosphere Pressure. Nanoscale 2010, 2, 559−563.

(11) McAllister, M. J.; Li, J.-L.; Adamson, D. H.; Schniepp, H. C.; Abdala, A. A.; Liu, J.; Herrera-Alonso, M.; Milius, D. L.; Car, R.; Prud'homme, R. K. Single Sheet Functionalized Graphene by Oxidation and Thermal Expansion of Graphite. Chem. Mater. 2007, 19, 4396−4404.

(12) Lv, W.; Tang, D. M.; He, Y. B.; You, C. H.; Shi, Z. Q.; Chen, X. C.; Chen, C. M.; Hou, P. X.; Liu, C.; Yang, Q. H. Low-Temperature Exfoliated Graphenes: Vacuum-Promoted Exfoliation and Electrochemical Energy Storage. ACS Nano 2009, 3, 3730−6.

(13) Steurer, P.; Wissert, R.; Thomann, R.; Mülhaupt, R. Functionalized Graphenes and Thermoplastic Nanocomposites Based Upon Expanded Graphite Oxide. Macromol. Rapid Commun. 2009, 30, 316−327.

(14) Voiry, D.; Yang, J.; Kupferberg, J.; Fullon, R.; Lee, C.; Jeong, H. Y.; Shin, H. S.; Chhowalla, M. High-Quality Graphene Via Microwave Reduction of Solution-Exfoliated Graphene Oxide. Science 2016, 353, 1413−1416.

(15) Grimm, S.; Schweiger, M.; Eigler, S.; Zaumseil, J. High-Quality Reduced Graphene Oxide by Cvd-Assisted Annealing. J. Phys. Chem. C 2016, 120, 3036−3041.

(16) Gao, W.; Ma, Y.; Zhang, Y.; Chen, Q.; Chen, H.; Zhu, B.; Jia, J.; Huang, A.; Xie, K.; Bai, Y. Architecture & Functionalization Evolution of Rgo Affect Physicomechanical Properties of Polyolefin/Rgo Composites. Composites, Part A 2018, 107, 479−488.

(17) Yun, Y. S.; Bae, Y. H.; Kim, D. H.; Lee, J. Y.; Chin, I. J.; Jin, H. J. Reinforcing Effects of Adding Alkylated Graphene Oxide to Polypropylene. Carbon 2011, 49, 3553−3559.

(18) Israelachvili, J. N. Chapter 3-strong Intermolecular Forces: Covalent and Coulomb Interactions. Intermol. & Surf. Forc. 2011, 53−70.

(19) Gao, W.; Lu, Y.; Chao, Y.; Ma, Y.; Zhu, B.; Jia, J.; Huang, A.; Xie, K.; Li, J.; Bai, Y. Performance Evolution of Alkylation Graphene Oxide Reinforcing High-Density Polyethylene. J. Phys. Chem. C 2017, 121, 21685−21694.

(20) Zhang, L.; Li, Y.; Wang, H.; Qiao, Y.; Chen, J.; Cao, S. Strong and Ductile Poly(Lactic Acid) Nanocomposite Films Reinforced with Alkylated Graphene Nanosheets. Chem. Eng. J. 2015, 264, 538−546.

(21) Vasileiou, A. A.; Kontopoulou, M.; Docoslis, A. A Noncovalent Compatibilization Approach to Improve the Filler Dispersion and Properties of Polyethylene/Graphene Composites. ACS Appl. Mater. Interfaces 2014, 6, 1916−1925.

(22) Hsiao, M. C.; Liao, S. H.; Lin, Y. F.; Wang, C. A.; Pu, N. W.; Tsai, H. M.; Ma, C. C. Preparation and Characterization of Polypropylene-Graft-Thermally Reduced Graphite Oxide with an Improved Compatibility with Polypropylene-Based Nanocomposite. Nanoscale 2011, 3, 1516−1522.

(23) Fang, Y.; Luo, B.; Jia, Y.; Li, X.; Wang, B.; Song, Q.; Kang, F.; Zhi, L. Renewing Functionalized Graphene as Electrodes for High-Performance Supercapacitors. Adv. Mater. 2012, 24, 6348−6355.
(24) Ye, X.; Qin, X.; Yan, X.; Guo, J.; Huang, L.; Chen, D.; Wu, T.; Shi, Q.; Tan, S.; Cai, X. Π−Π Conjugations Improve the Long-Term Antibacterial Properties of Graphene Oxide/Quaternary Ammonium Salt Nanocomposites. Chem. Eng. J. 2016, 304, 873−881.
(25) García, M. T.; Campos, E.; Ribosa, I. Biodegradability and Ecotoxicity of Amine Oxide Based Surfactants. Chemosphere 2007, 69, 1574−1578.
(26) Pallon, L. K. H.; Hoang, A. T.; Pourrahimi, A. M.; Hedenqvist, M. S.; Nilsson, F.; Gubanski, S.; Gedde, U. W.; Olsson, R. T. The Impact of Mgo Nanoparticle Interface in Ultra-Insulating Polyethylene Nanocomposites for High Voltage Dc Cables. J. Mater. Chem. A 2016, 4, 8590−8601.
(27) Compton, O. C.; Dikin, D. A.; Putz, K. W.; Brinson, L. C.; Nguyen, S. T. Electrically Conductive "Alkylated" Graphene Paper Via Chemical Reduction of Amine-Functionalized Graphene Oxide Paper. Adv. Mater. 2010, 22, 892−896.
(28) Becerril, H. A.; Mao, J.; Liu, Z.; Stoltenberg, R. M.; Bao, Z.; Chen, Y. Evaluation of Solution-Processed Reduced Graphene Oxide Films as Transparent Conductors. ACS Nano 2008, 2, 463−70.
(29) Raccichini, R.; Varzi, A.; Wei, D.; Passerini, S. Critical Insight into the Relentless Progression toward Graphene and Graphene-Containing Materials for Lithium-Ion Battery Anodes. Adv. Mater. 2017, 29, 1603421.
(30) Si, Y.; Samulski, E. T. Synthesis of Water Soluble Graphene. Nano Lett. 2008, 8, 1679−1682.
(31) Alig, I.; Pötschke, P.; Lellinger, D.; Skipa, T.; Pegel, S.; Kasaliwal, G. R.; Villmow, T. Establishment, Morphology and Properties of Carbon Nanotube Networks in Polymer Melts. Polymer 2012, 53, 4−28.
(32) Donohue, M. D.; Aranovich, G. L. Classification of Gibbs Adsorption Isotherms. Adv. Colloid Interface Sci. 1998, 76−77, 137−152.
(33) Zhang, Y.; Lam, F. L.; Hu, X.; Yan, Z. Formation of an Ink-Bottle-Like Pore Structure in Sba-15 by Mocvd. Chem. Commun. 2008, 41, 5131−5133.
(34) Song, M. Y.; Cho, S. Y.; Kim, R. K.; Jung, S. H.; Lee, J. K.; Yun, Y. S.; Jin, H. J. Alkylated and Restored Graphene Oxide Nanoribbon-Reinforced Isotactic-Polypropylene Nanocomposites. Carbon 2016, 108, 274−282.
(35) Ryu, S. H.; Shanmugharaj, A. M. Influence of Long-Chain Alkylamine-Modified Graphene Oxide on the Crystallization, Mechanical and Electrical Properties of Isotactic Polypropylene Nanocomposites. Chem. Eng. J. 2014, 244, 552−560.
(36) Meng, W.; Gall, E.; Ke, F.; Zeng, Z.; Kopchick, B.; Timsina, R.; Qiu, X. Structure and Interaction of Graphene Oxide− Cetyltrimethylammonium Bromide Complexation. J. Phys. Chem. C 2015, 119, 21135−21140.
(37) Russat, J. Characterization of Polyamic Acid/Polyimide Films in the Nanometric Thickness Range from Spin-Deposited Polyamic Acid. Surf. Interface Anal. 1988, 11, 414−420.
(38) Cheng, H. K. F.; Sahoo, N. G.; Tan, Y. P.; Pan, Y.; Bao, H.; Li, L.; Chan, S. H.; Zhao, J. Poly(Vinyl Alcohol) Nanocomposites Filled with Poly(Vinyl Alcohol)-Grafted Graphene Oxide. ACS Appl. Mater. Interfaces 2012, 4, 2387−2394.
(39) Pourrahimi, A. M.; Hoang, T. A.; Liu, D.; Pallon, L. K. H.; Gubanski, S.; Olsson, R. T.; Gedde, U. W.; Hedenqvist, M. S. Highly Efficient Interfaces in Nanocomposites Based on Polyethylene and Zno Nano/Hierarchical Particles: A Novel Approach toward Ultralow Electrical Conductivity Insulations. Adv. Mater. 2016, 28, 8651−8657.
(40) Hsiao, M.-C.; Liao, S.-H.; Lin, Y.-F.; Wang, C.-A.; Pu, N.-W.; Tsai, H.-M.; Ma, C.-C. M. Preparation and Characterization of Polypropylene-Graft-Thermally Reduced Graphite Oxide with an Improved Compatibility with Polypropylene-Based Nanocomposite. Nanoscale 2011, 3, 1516−1522.
(41) Kumar, P.; Yu, S.; Shahzad, F.; Hong, S. M.; Kim, Y. H.; Koo, C. M. Ultrahigh Electrically and Thermally Conductive Self-Aligned Graphene/Polymer Composites Using Large-Area Reduced Graphene Oxides. Carbon 2016, 101, 120−128.
(42) Wakabayashi, K.; Pierre, C.; Dikin, D. A.; Ruoff, R. S.; Ramanathan, T.; Brinson, L. C.; Torkelson, J. M. Polymer-Graphite Nanocomposites: Effective Dispersion and Major Property Enhancement Via Solid-State Shear Pulverization. Macromolecules 2008, 41, 1905−1908.
(43) Choi, J. T.; Kim, D. H.; Ryu, K. S.; Lee, H.-i.; Jeong, H. M.; Shin, C. M.; Kim, J. H.; Kim, B. K. Functionalized Graphene Sheet/Polyurethane Nanocomposites: Effect of Particle Size on Physical Properties. Macromol. Res. 2011, 19, 809−814.
(44) Qian, D.; Dickey, E. C.; Andrews, R.; Rantell, T. Load Transfer and Deformation Mechanisms in Carbon Nanotube-Polystyrene Composites. Appl. Phys. Lett. 2000, 76, 2868−2870.
(45) Yuan, B.; Bao, C.; Song, L.; Hong, N.; Liew, K. M.; Hu, Y. Preparation of Functionalized Graphene Oxide/Polypropylene Nanocomposite with Significantly Improved Thermal Stability and Studies on the Crystallization Behavior and Mechanical Properties. Chem. Eng. J. 2014, 237, 411−420.
(46) Wei, P.; Bai, S. Fabrication of a High-Density Polyethylene/Graphene Composite with High Exfoliation and High Mechanical Performance Via Solid-State Shear Milling. RSC Adv. 2015, 5, 93697−93705.

DOI: 10.1021/acs.jpcc.7b12787
J. Phys. Chem. C 2018, 122, 7968−7974